A ROUND ROBIN TEST OF FLASH THERMOGRAPHY OF CFRP AND METAL STRUCTURES

Nick ROTHBART [1], Christiane MAIERHOFER [1], Matthias GOLDAMMER [2], Felix HOHLSTEIN [3], Joachim KOCH [4], Igor KRYUKOV [5], Guido MAHLER [6], Bernhard STOTTER [7], Günter WALLE [8], Beate OSWALD-TRANTA [9], Martin SENGEBUSCH [10]

[1] Federal Institute for Materials Research and Testing (BAM), Berlin, Germany
[2] Siemens AG Corporate Technology, München, Germany
[3] Block Materialprüfung GmbH, Berlin, Germany
[4] edevis GmbH, Stuttgart, Germany
[5] University of Kassel, Kassel, Germany
[6] InfraTec GmbH Infrarotsensorik und Messtechnik,
[7] University of Applied Science Upper Austria, Wels, Austria
[8] Fraunhofer Institute for Nondestructive Testing IZFP, Saarbrücken, Germany
[9] University of Leoben, Leoben, Austria
[10] Deutsches Institut für Normung e. V.

Abstract. Within the scope of a DIN INS project, a flash thermography round robin test that evaluates reliability, comparability and efficiency of different testing situations is organized. The results give information about the detectability of defects e.g. by their size and depth, the evaluation method and by the materials used. Besides, the influence of equipment and parameters used by the participants on the results were analysed. All of the quantitative results as well as the feedback given by the participants will be presented in a DIN committee in order to contribute to a flash thermography standard.

1. Introduction

With flash thermography a fast and sensitive non-destructive testing method for CFRP and metal structures is available that reveals great potential for the integration into production processes. The high detection sensitivity of defects which are situated close to the surface and which are orientated parallel to it allows e.g. the detection of delamination and voids. Thus, the method can be applied for efficient testing of adhesive bondings, coatings and fibre reinforced composite structures [1]. Other common applications are concerning metallic structures, e.g. the quality assurance of spot and laser welding joints [2], the detection of oblique cracks and overlaps and the control of soldered joints [3]. Frequently, flash thermography can be used complementary to other NDT method. Despite the great potential of active thermography, there is still a lack of testing standards, reference test specimen and round robin tests, which are required for harmonizing the testing procedure.

The only known round robin tests for active thermography were conducted in 1998 and 2000 using CFRP specimens with impact damage [4, 5]. The aim of the trials of the former Eurotherm working group was the comparison of different excitation and evaluation techniques of active thermography by assessing the signal-to-noise ratio (SNR) of the detected flaws and other performance characteristics. Among other thermographic excitation methods, also flash thermography was evaluated. In the first tests, investigations of a 2 mm thick sample showed that optical excitation using longer heating steps resulted in the highest SNR values, while flash thermography reached a higher spatial resolution. Only data evaluation using pulse phase thermography (PPT) [6] yielded to comparable SNR values of flash thermography data.

In the second round robin test, specimens with thicknesses of up to 7 mm were examined. Here, none of the optical excitation methods including flash thermography could detect the entire impact damage from the front side. This was only possible using ultrasonic excitation.

For the correct application of flash thermography, in 2007 an ASTM standard was published titled ASTM E 2582-07 „Standard Practice for Infrared Flash Thermography of Composite Panels and Repair Patches Used in Aerospace Applications“. Here, the testing procedure as well as the data analysis is described in detail, but quantitative information concerning the appropriate excitation energy and further measurement parameters are missing. Also the limitations of the methods like penetration depth and detection sensitivity are not considered.

Therefore, in the following new round robin tests are described, which are demonstrating the accuracy and precision of flash thermography as a validation study in accordance with DIN EN ISO/IEC 17043:2010-05. Simultaneously, these tests should provide comparable information upon the performance of different test equipment. Thus, 16 test specimens were planned and constructed consisting of different metals (steel, copper and aluminium) and of CFRP with various artificial and natural defects. These test specimens are presenting different testing situations and are enabling a qualitative and partially quantitative evaluation of the results. The tasks have been specified by an extensive measurement programme. A selection of the achieved results is presented in the following.

2. Measurement programme

2.1 Participants of the round robins tests and equipment

Nine institutions from different backgrounds participated in the round robin tests. These included universities, research institutes, industrial companies and small and medium enterprises. Together with the DIN e. V. as project manager, they are listed in the authorship. Table 1 summarizes the equipment and measurement parameters of all participants related to the investigations performed at the large steel test specimen (200 x 200 x 7.5 mm³) containing flat bottom holes (see chapter 2.2).

For thermal excitation, one to two flash lamps with flash durations from 1 to 11 ms were used. Total energies between 6 and 24 kJ were converted. With this energy, the measured temperature rise of a defined sensor plate was between 0.8 and 24 K. By considering the known heat capacity of this sensor plate (0.242 J/K) and its surface size of 1 cm², this corresponds to an input energy density between 0.2 and 5.8 J/cm².

With the exception of one microbolometer infrared (IR) camera, all IR cameras used contain an indium antimonite (InSb) sensor with 320 x 256 to 640 x 512 pixels. As

sensitive wavelength areas, all InSb cameras lay within the MWIR range between 1.5 to 5.7 µm. For the investigations at the steel test specimen, frame rates between 50 Hz (recommended frame rate) and 353 Hz were selected. The integration times were set between 720 and 2500 µs resulting in temperature resolutions (noise equivalent temperature difference NETD) between 40 and 18 mK. The geometry of the experimental set-up was not very different for all participants. The distances of the flash lamps to the sample and of the IR camera to the sample were varying between 24 and 80 cm and between 33 and 81 cm, respectively. The angles of the flash lamps to the normal of the sample surfaces were set between 0 and 45°.

Table 1. Applied equipment and parameters related to the investigations of the large V2A test specimen.

participant	A	B	C	D	E	F	G	H	I
flash									
energy	4 x 6 kJ	2 x 6.4 kJ	2 x 3 kJ	2 x 3 kJ	1 x 6 kJ	2 x 3 kJ	1 x 6 kJ	1 x 6 kJ	1 x 6 kJ
duration	2.6 ms	10 ms	2 ms	k. A.	11 ms	2 ms	10 ms	8 ms	1 ms
distance	30 cm	25 cm	30 cm	24 cm	36 cm	50 cm	35 cm	35 cm	80 cm
angle	15°	45°	30°	41°	40°	30 °	30°	0°	10°
ΔT (see text)	k. A.	8 K	11 K	4.2 K	k. A.	24 K	13.6 K	0.8 K	9 K
energy input	k. A.	1.9 J/cm²	2.6 J/cm²	1.0 J/cm²	k. A.	5.8 J/cm²	3.3 J/cm²	0.2 J/cm²	2.2 J/cm²
IR camera									
type of detector	InSb	InSb	InSb	micro-bolo-meter	InSb	InSb	InSb	InSb	InSb
wavelength interval	2 – 5 µm	2.5 – 5.1 µm	3 – 5 µm	7.5 – 14 µm	1.5 – 5.4 µm	3 – 5 µm	3 – 5 µm	3.5 – 5.7 µm	1.5 – 5.1 µm
array size	640 x 512	320 x 256	320 x 256	384 x 288	640 x 512	640 x 512	640 x 512	640 x 512	320 x 256
frame rate	50 Hz	50 Hz	300 Hz	50 Hz	353 Hz	100 Hz	50 Hz	200 Hz	50 Hz
integration time	720 µs	800 µs	1000 µs	k. A.	2200 µs	2500 µs	2500 µs	1560 µs	1500 µs
NETD	< 25 mK	30 mK	< 20 mK	< 40 mK	18 mK	20 mK	< 20 mK	45 mK	< 20 mK
distance	65 cm	70 cm	70 cm	49 cm	64 cm	48 cm	67 cm	33 cm	81 cm
lens	25 mm	27 mm	M25	25 mm	25 mm	25 mm	20° x 16° FOV	12 mm	25 mm

2.2 Test specimens

Within the round robin tests, in total 16 test specimens made of different materials and consisting various defects were investigated. The design of the test specimens was based mainly on results obtained in the TNS project Flash Thermography [7]. Among others, these consist of three large (200 x 200 x 7.5 mm³) and three small (100 x 100 x 4.5 mm³) metal test specimens made of aluminium, copper and stainless steel (V2A) with flat bottom holes of different sizes. The diameters of the holes were between 8 and 32 mm for the large and between 1 and 4 mm for the small test specimens, the remaining wall thicknesses were between 2 and 6 mm and between 0.2 and 3.5 mm, respectively. Fig. 1 shows the large and the small V2A test specimens, which will be discussed in the following. Further on, as test specimens a quasiisotropic CFRP plate with a size of 200 x 200 x 6 mm³ and with flat bottom holes, two plates made of V2A and copper with crossed notches and a notch wedge

(80 x 70 x 6 mm³), a CFRP stepped wedge with artificial delaminations made of PTFE (200 x 200 x 1.5 to 3.5 mm³), and three plates made of quasiisotropic CFRP and three plates made of unidirectional CFRP, each set with defined impact damages between 2.5 and 10 J (low velocity impact) were investigated. After construction, all test specimens were analysed first with the equipment at BAM. For the metal test specimens, a blackening of the surfaces was suitable using graphite spray for enhancing the emissivity. This graphite spray was recommended to be used by all participants during the round robin tests.

Fig. 1. Backside of the V2A test specimens with sizes of 200 x 200 x 7.5 mm³ (left) and of 100 x 100 x 4.5 mm³ (right) with flat bottom holes with different diameters and remaining wall thicknesses.

2.3 Inspection tasks

The inspection tasks of the round robin tests contained measurements with flash thermography at all test specimens and in most cases in reflection configuration. Only some of the CFRP test specimens were also investigated in transmission configuration. Different steps in data analyses at selected thermograms and phase images were specified. The V2A test specimens described above were investigated as described in the following:

- Verification of the homogeneity of the illumination using a paper wall and determination of the input energy density by measuring the temperature rise of a supplied sensor plate
- Selection of thermograms from the recorded cooling down sequences providing an optimum thermal contrast of the defects
- Application of pulse phase thermography (PPT) and selection of suited phase images
- Documentation of the detectability and determination of the signal to noise ratio (SNR) of all defects in the selected thermograms and phase images. Here, the signal intensity is equal to the maximum temperature or phase difference, and the noise is calculated from the standard deviation of the temperature or phase values inside an undisturbed area of the test specimen.
- Measurement of the diameters of the holes inside the thermograms and determination of the time, where the holes are appearing in the thermograms with the maximum thermal contrast

For the other test specimens, the inspection tasks included the documentation of the number of detected defects depending on their size and remaining wall thickness or depth (flat bottom holes, delaminations), the determination of the spatial resolution (crossed notches) and penetration depth (notch wedge), and the determination of the size of the impact damage. For all inspection tasks, detailed test instructions were given containing

recommended measurement parameters and test protocol templates for the documentation of measurement parameters and results. Among others, detailed instructions were given for the determination of SNR values and for homogeneous blackening of the metal samples.

3. Results of the steel test specimen

3.1 Influence of defect geometry

For a quantitative evaluation of the influence of defect geometry, the number of detected defects and the SNR of all defects were determined for both V2A test specimens. Fig. 2 shows how often each hole could be detected by the nine participants. While the holes with a diameter of 32 mm and remaining wall thicknesses from 2 to 4 mm could be detected by all participants, the hole with a diameter of 1 mm and a remaining wall thickness of 1.5 mm could be detected only by six participants. The less detectability of deeper holes can be explained by the limited penetration depth within the model of thermal waves. Holes with smaller diameters are detected less often (for similar remaining wall thicknesses), as the contrast is reduced by lateral heat diffusion processes.

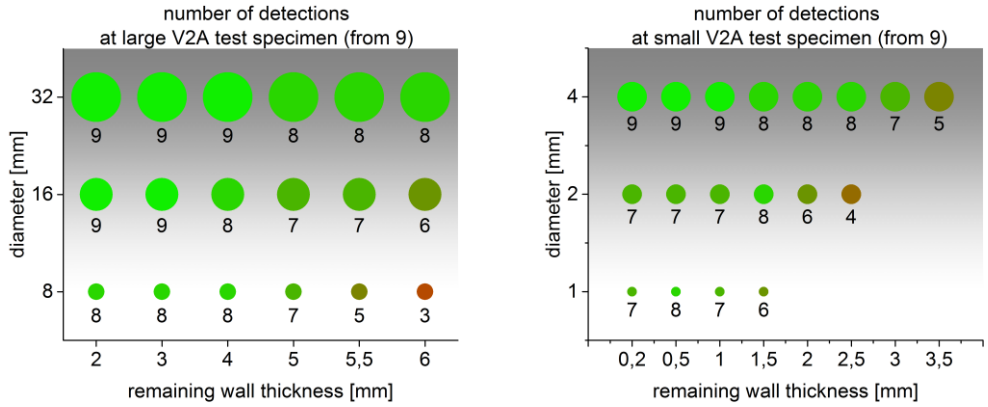

Fig. 2. Number of detections (from nine) of the flat bottom holes inside the phase images as a function of the diameter and the remaining wall thickness. Larger holes close to the surface could be detected more often.

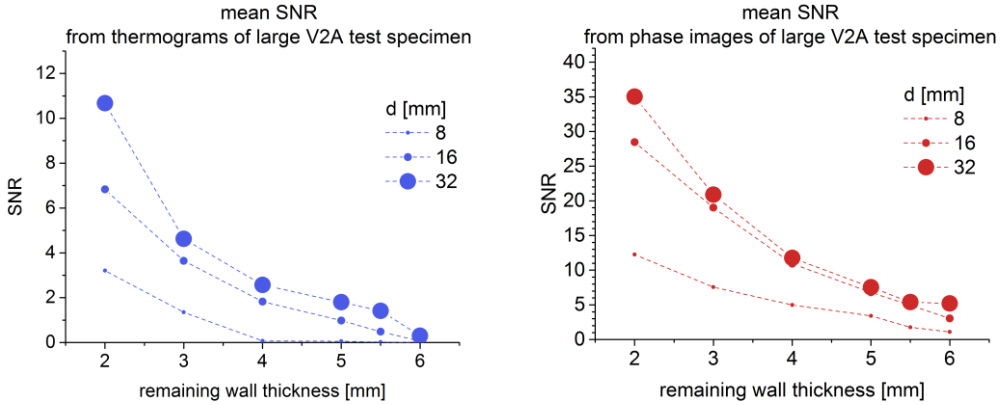

Fig. 3. SNR of the different hole geometries inside the thermograms (left) and the phase images (right) at the large V2A test specimen. The values are averaged using the data from all participants.

This relationship is confirmed by the data shown in fig. 3. Here, the SNR values averaged for all participants are depicted for different diameters as a function of the remaining wall thickness for the thermograms (left) as well as for the phase images (right) for the large V2A test specimen. In both cases, large diameters as well as a small remaining wall thicknesses are contributing to a high SNR value and thus to a high detectability. Not directly from the diagrams, but obvious from the data it can be concluded that for similar

aspect ratios, holes with a smaller diameter could be detected with a higher SNR. This can be explained by the limited penetration depth. Further on, the comparison of both diagrams clearly shows that the phase images are imaging the holes with a significant higher SNR as the thermograms (see also chapter 3.2).

Fig. 4 shows the diameters of the holes, which were determined by the full width at half maximum (FWHM) of the signals in the thermograms. The results of each participant are depicted with a different colour. It becomes obvious that the scattering of the measured data among the participants is very large. The relative range of the data goes up to 125 % related to the nominal diameter. Therefore, an objective determination of the diameter from the thermograms is difficult. The time after the flash, at which the thermogram was recorded, has an influence and should be documented. Also the values of similar diameters determined by each individual participant are scattering strongly, as the holes are having different depth and thus are influenced by lateral heat diffusion processes in different ways.

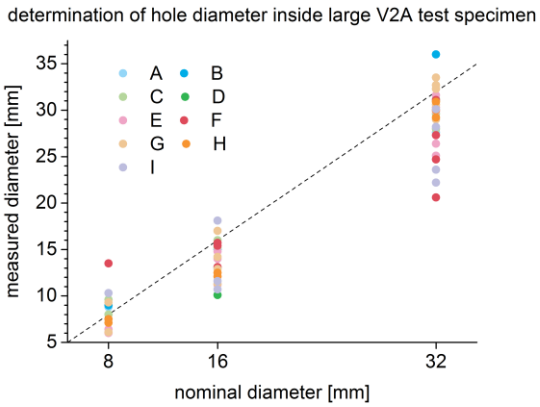

Fig. 4. Relationship between the nominal diameters and the diameters which were measured inside the thermograms by each participant at the large V2A test specimen. The scattering of the measured values is relatively large.

3.2 Influence of the evaluation method

Also the influence of the applied method used for data evaluation was investigated using the large V2A test specimen. As described above, the SNR of the holes measured in the thermograms as well as in the phase images of the PPT were compared.

Fig. 5 shows thermograms (top) and phase images (bottom) of three different participants. For each thermogram and for each phase image, the time of recording and the frequency are given, respectively. In all cases, the phase images are delivering better results, as the holes can be recognized more clearly. The images of participant D (left) show a very high noise and especially in the thermogram, an inhomogeneous heating can be observed. Thus, in the phase image only five holes could be detected. In contrast to that, in the phase image of participant E (right), all 18 holes could be seen. Here, in the signatures of some of the larger holes an inversion of the phase contrast from light/dark to dark/light could be observed.

For a quantitative proof of the observations described above, fig. 6 shows the number of detected holes from a total of 18 holes (left) as well as the mean SNR of all holes (right) for the thermograms and for the phase images of the large V2A test specimen. Holes, which could not be detected, were rated by an SNR of 0. In the diagrams, the individual results of each participant are depicted with different colours. Additionally, the mean values from all participants are displayed as wide bars. It is shown clearly and in consistence with all participants, that the phase images are delivering the better results (see also fig. 3).

On average, about 11 holes could be detected in the thermograms, while in the phase images 16 holes are found. The mean SNR of the phase images with a value of about 11 is about four times larger as the mean SNR of the thermograms (about 2.5). It becomes evident that the scattering of the individual results is larger in the phase images as in the thermograms. The reason could be the large number of variables, which could be selected for the calculation of the phase images using the thermal sequences by PPT and which were not recommended in advance.

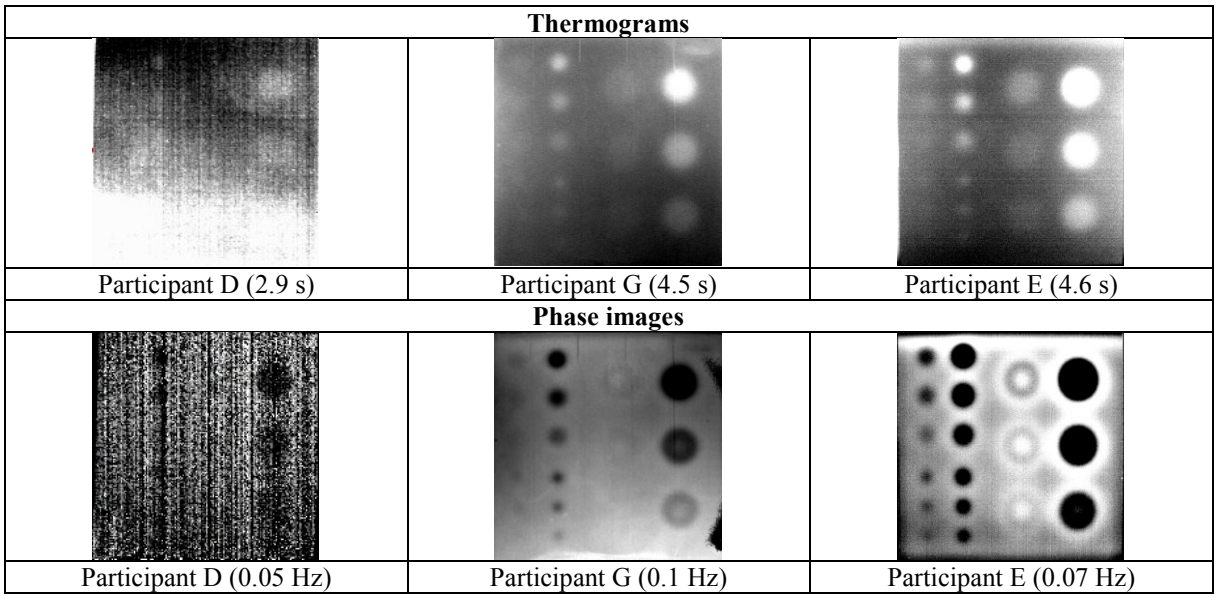

Fig. 5. Selected thermograms (top) and phase images (bottom) of different participants. The quality of the images is different, while obviously the phase images show the better results.

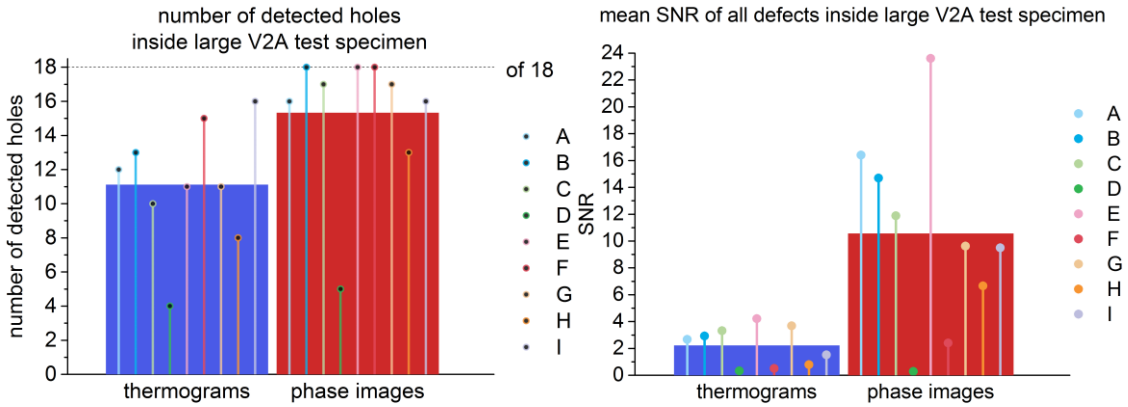

Fig. 6. Representation of the mean numbers of the detected flaws (left) and of the mean SNR (right) of the flaws in the thermograms and phase images of the large V2A test specimen. Coincidentally, more flaws with higher SNR can be detected in the phase images.

4. Conclusion

In this paper, as a selection from the whole round robin tests the results of two test specimen consisting of stainless steel have been presented. As different equipment configurations have been used by the participants, the obtained results are scattering widely. Due to the high amount of parameters and due to the deviating results in the different measurement tasks, it is difficult to obtain general statements about the influence of single parameters. However, it can be seen that the lowest SNR is correlated with the

highest NETD and the lowest energy input. Thus, these parameters are highly important for achieving a high SNR. A low NETD can be realized by using a sensitive detector and the longest possible integration time. And a high energy input into the material is reached by using flash lamps with a high flash energy in a distance to the sample as closest as possible.

By comparing thermograms and phase images, the phase images show a stronger scattering of the results, as multiple parameters like the length of the sequences, the frame rate or the start time of the FFT have an influence on the results of pulse phase thermography (PPT). But in summary, in the phase images more holes could be detected with a higher SNR as in the thermograms.

Furthermore, the influence of hole geometry was analysed systematically, which allows an estimation of the detection limits. Here, most of the investigated holes could be detected. Only four flat bottom holes with a diameter of 1 mm and remaining wall thicknesses of larger than 1.5 mm could not be detected. Smaller and deeper holes could be detected less often. The smallest flat bottom hole with a diameter of 1 mm and a remaining wall thickness of 1.5 m could be detected only by six participants.

Acknowledgements

The project was funded within the programme **Innovations with Norms and Standards** (INS 1255) by the Federal Ministry of Economics and Energy. Within DIN e. V., the Standards Committee Materials Testing (NMP) was responsible for the project.

References

[1] Maierhofer, C., Röllig, M., Ehrig, K., Meinel, D., Céspedes-Gonzales, G.; Validation of flash thermography using computed tomography for characterizing inhomogeneities and defects in CFRP structures. *Composites Part B: Engineering*, Volume 64, August 2014, Pages 175-186

[2] Jonietz, F., Ziegler, M., Philipp Myrach, P., Suwala, H., Rethmeier, M.; Untersuchung von Punktschweißverbindungen mit aktiver Thermografie. DGZfP Tagungsband zur DACH-Tagung 2015, im Druck

[3] Maierhofer, C., Röllig, M., Steinfurth, H., Ziegler, M., Kreutzbruck, M., Scheuerlein, C., Heck, S.; Non-destructive testing of Cu solder connections using active thermography. *NDT&E International* 52 (2012) 103–111.

[4] Vavilov, V. P., Almond, D. P., Busse G., Grinzato E., Krapez J-C.,Maldague X., Marinetti, S., Peng, W., Shirayev, V., Wu, D.: Infrared thermographic detection and characterisation of impact damage in carbon fiber composites: results of the round robin test. QIRT 1998, Lodz, Poland

[5] Almond, D. P., Ball, R. J., Dillenz, A., Busse, G., Krapez, J.-C., Galmiche, F., Maldague X.: Round Robin comparison II of the capabilities of various thermographic techniques in the detection of defects in carbon fibre composites. QIRT 2000, http://qirt.gel.ulaval.ca/archives/qirt2000/papers/065.pdf

[6] Maldague, X., Galmiche, F., Ziadi, A.; Advances in pulsed phase thermography. *Infrared Physics & Technology* 43 (2002) 175–181.

[7] Maierhofer, C., Myrach, P., Ziegler, M., Krankenhagen, R., Steinfurth, H., Reischel, M.; Abschlussbericht zum Vorhaben Entwicklung von Normen und Standards für die aktive Thermografie mit Blitzlichtanregung; Berlin, Hannover Technische Informationsbibliothek u. Universitätsbibliothek, August 2013, http://edok01.tib.uni-hannover.de/edoks/e01fb15/815242689.pdf